ELSEVIER

Materials Science and Engineering A222 (1997) 76–83

MATERIALS SCIENCE & ENGINEERING A

The effect of Al on mechanical properties and microstructures of Fe–32Mn–12Cr–xAl–0.4C cryogenic alloys

Young S. Han, Soon H. Hong*

Department of Materials Science and Engineering, Korea Advanced Institute of Science and Technology, 373-1 Kusung-dong, Yusung-gu, Taejon 305-701, South Korea

Received 30 October 1995; revised 24 June 1996

Abstract

The effect of Al addition (0–3 wt%) on tensile properties and microstructures of Fe–32Mn–12Cr–xAl–0.4C cryogenic alloys were investigated at temperatures ranging from −196 to 250°C. The Al is an austenite stabilizer suppressing the formation of the strain induced ε-martensite, while it behaved as a δ-ferrite stabilizer when added to 3 wt%. The Fe–32Mn–12Cr–0Al–0.4C alloy showed the strain induced ε-martensite after tensile deformation at −196°C. Deformation twins were observed in deformed cryogenic alloys except Fe–32Mn–12Cr–2Al–0.4C alloys at temperatures ranging from −196 to 25°C. The formation of both the deformation twins and the strain induced ε-martensite enhanced the tensile elongation by retarding local necking. The Fe–32Mn–12Cr–(0,1,3)Al–0.4C alloys exhibited elongation peaks within a temperature range forming the deformation twins. As the stacking fault energy increases with increasing Al content, the elongation peak shifted to lower temperature with increasing Al content in Fe–32Mn–12Cr–xAl–0.4C alloy. The continuous formation of strain induced phases, deformation twins and ε-martensite, up to a large strain was important to increase the tensile elongation of Fe–32Mn–12Cr–xAl–0.4C cryogenic alloys.

Keywords: Cryogenic alloys; ε-martensite; Tensile elongation; Deformation twins

1. Introduction

The most commonly used cryogenic alloys are the austenitic stainless steels and 9% Ni steel for liquefied natural gas (LNG) storage applications at −162°C [1]. These alloys have relatively high nickel content to improve the toughness at cryogenic temperature and thus the costs are high due to the high nickel content. In order to lower the production cost, manganese has been considered as a substituting element for nickel in cryogenic alloys. Developmental researches on the Fe–Mn–Cr alloys have been carried out in USA, Japan, and USSR since the early 1970s. These included a joint Soviet–American research project on materials for storage and transport of LNG which has led to the development of austenitic alloys based on 19Mn–13Cr with low interstitial content 0.03 wt.% C and 0.02 wt.% N [2]. Since the 1980s, the austenitic Fe–Mn–Al alloys were also developed for cryogenic applications [3,4]. Kim et al. [4] reported the development of Fe–30Mn–5Al–0.3C–0.1Nb alloy with high strength and excellent toughness.

The plastic deformation of high manganese austenitic alloys is known to induce the formation of deformation twins, ε-martensite and α'-martensite in austenitic phases depending on the chemical compositions and test temperature. The mechanical properties of high manganese austenitic alloys are sensitively dependent on the formation of strain induced features, since the strain induced features affect the neck propagation during tensile deformation [5–7]. Particularly, the total amounts and formation rates of strain induced features during plastic deformation greatly affect the strain hardening rates of these alloys [8]. The formation of strain induced features is closely related to the stability of austenite which is dependent on the stacking fault energy [9].

In this study, the effects of aluminum addition (0–3 wt.%) to Fe–32Mn–12Cr–xAl–0.4C cryogenic alloys on tensile properties and microstructures were investigated from −196 to 250°C. Since the aluminum addition in high manganese austenitic alloys increases the

* Corresponding author.

PII S0921-5093(96)10501-3

Table 1
The nominal and analyzed compositions of melted Fe–32Mn–12Cr–xAl–0.4C alloys

Alloy designation	Nominal composition (wt.%)					Analysed composition (wt.%)				
	Fe	Mn	Cr	Al	C	Fe	Mn	Cr	Al	C
0-Al	Bal.	32	12	0	0.4	Bal.	31.9	12.3	—	0.4
1-Al	Bal.	32	12	1	0.4	Bal.	32.8	12.1	0.6	0.3
2-Al	Bal.	32	12	2	0.4	Bal.	31.7	12.1	2.1	0.4
3-Al	Bal.	32	12	3	0.4	Bal.	32.2	12.1	2.6	0.4

stability of the austenitic phase, the tendency to form the strain induced features is expected to be changed with the aluminum content. This work is intended to clarify the effect of aluminum on mechanical properties and deformed microstructures. The characteristics on the formation of strain induced features, i.e. deformation twins and ε-martensite, were analyzed through the calculation of stacking fault energies. The effects of the strain induced phases on strain hardening rate are used to explain the variation of tensile elongation of Fe–32Mn–12Cr–xAl–0.4C cryogenic alloys.

2. Experimental procedures

Four Fe–32Mn–12Cr–xAl–0.4C alloys with different Al contents were prepared by induction melting and the compositions were analyzed by atomic adsorption spectrometry as shown in Table 1. The cast ingots of 60 mm thickness were homogenized at 1150°C for 2 h and then hot-rolled into 4 mm thick plates. Plate type tensile specimens with thickness of 3 mm and gauge length of 30 mm were machined from the hot-rolled plates. The specimens were solution treated at 1050°C for 2 h in argon atmosphere and followed by water-quenching. The tensile tests were performed at temperatures ranging from −196 to 250°C with an initial strain rate of 5.6×10^{-4} s^{-1}.

X-ray diffraction analyses were performed using a CuKα radiation to determine the existing phases at test temperatures. The volume fraction of δ-ferrite phase was measured by magnetic saturation measurement using a ferrite scope (Model: MP3). The microstructures of the specimens before and after the tensile test were examined by optical microscopy and transmission electron microscopy. The optical micrographs were taken after electrolytic etching of the polished surfaces with a saturated oxalic acid solution. Thin foils for transmission electron microscopy were prepared by the jet polishing technique using a solution of 10% perchloric acid and 90% acetic acid at 25°C.

3. Results and discussion

3.1. Microstructures

Fig. 1 shows the X-ray diffraction patterns of the Fe–32Mn–12Cr–xAl–0.4C alloys before and after the tensile test at −196°C. The 0-Al, 1-Al and 2-Al alloys showed a single austenite phase before the tensile test, while the 3-Al alloy showed a δ-ferrite phase in addition to the austenite phase as shown in Fig. 1(a). Comparing the X-ray diffraction patterns before the tensile test (Fig. 1(a)) with those after the tensile test (Fig. 1(b)), there were no microstructural change after tensile deformation at −196°C in 1-Al, 2-Al and 3-Al alloys. However, the X-ray diffraction peaks of 0-Al alloy showed the peaks from ε-martensite in addition to the peaks from austenite after tensile test at −196°C. This indicates the ε-martensite is a strain induced phase formed during tensile deformation of 0-Al alloy at −196°C. Table 2 shows the results of the phase analyses from the X-ray diffraction of Fe–32Mn–12Cr–xAl–0.4C alloys before and after tensile test at −196, −130 and 25°C, respectively. The results of the phase analyses in Table 2 indicate that there is no microstructural change during tensile deformation at −130 and 25°C in all tested alloys. The X-ray diffraction patterns from the 0-Al alloy after tensile tested at temperatures above −130°C did not show the ε-martensite. Therefore, it is considered that the maximum temperature of the strain induced ε-martensite formation during the deformation, E_d, exists between −130 and −196°C. These results show that the stability of austenite phase in Fe–32Mn–12Cr–xAl–0.4C alloys sensitively depends on the aluminum content. The addition of aluminum in Fe–32Mn–12Cr–0.4C alloys stabilized the austenite phase against the ε-martensite. However, aluminum act as a δ-ferrite stabilizer in Fe–32Mn–12Cr–xAl–0.4C alloy. The Fe–32Mn–12Cr–2.6Al–0.4C alloy exhibited $\gamma + \delta$ phases, while the Fe–32Mn–12Cr–2.1Al–0.4C alloy exhibited a γ single phase. It is considered that the δ phase is stabilized when the Al content is at least higher than 2.6 wt.% in the Fe–32Mn–12Cr–xAl–0.4C alloy.

Fig. 2 shows the microstructures before and after tensile test of Fe–32Mn–12Cr–xAl–0.4C alloy at

25°C. Fig. 2(a) and (c) are the optical micrographs of 0-Al and 1-Al alloys before tensile test at 25°C. Fig. 2(b) and (d) are the optical micrographs of 0-Al and 1-Al alloys after tensile test at 25°C. Fig. 2(b) and (d) show the formation of a new strain induced feature during tensile deformation, which was not detectable by X-ray diffraction analysis in Table 2. Fig. 2(e) shows dark field image of the strain induced feature observed by transmission electron microscope in 0-Al alloy after tensile test at 25°C. The new feature was identified as deformation twins having a twin plane of $(\bar{1}1\bar{1})$ from the analysis of the electron diffraction pattern shown in Fig. 2(f). The deformation twins were formed in deformed 3-Al alloy, but were not observed in deformed 2-Al alloy.

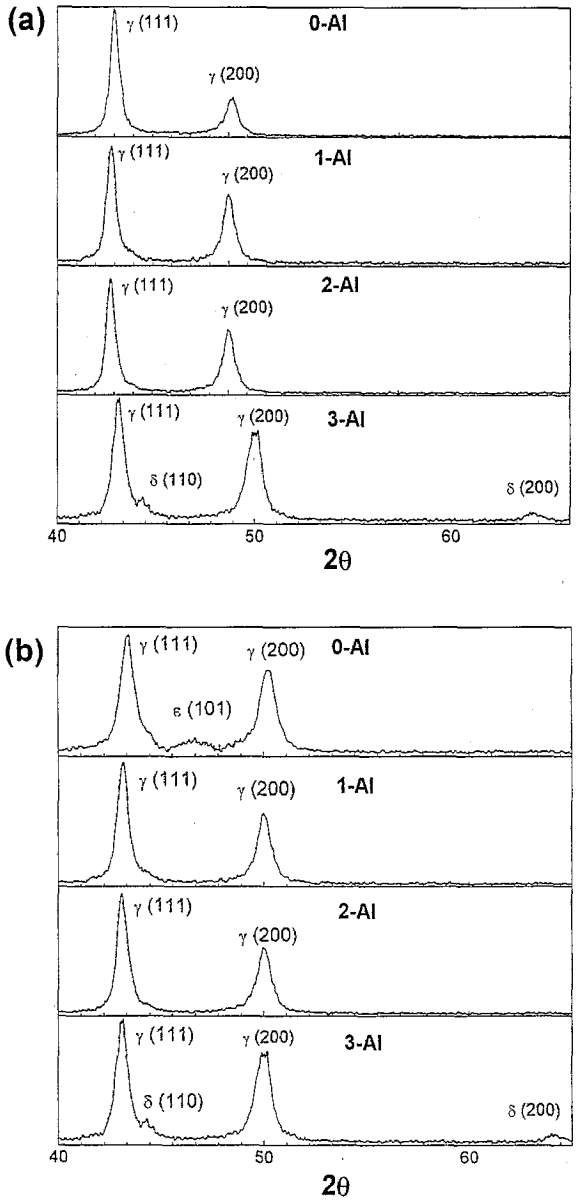

Fig. 1. The X-ray diffraction patterns of the Fe–32Mn–12Cr–xAl–0.4C alloys tested at −196°C : (a) before tensile test, (b) after tensile test.

3.2. Stacking fault energy

The effects of composition and temperature on strain induced phase formation of deformation twins and ε-martensite in austenitic steels were known to be strongly related to the stacking fault energy [10]. As the stability of austenite phase decreases with decreasing stacking fault energy, the tendency to form the strain induced features increases with decreasing stacking fault energy. The austenitic steels with lower stacking fault energy were reported to form the ε-martensite preferentially to deformation twinning in Fe–Cr–Ni and Fe–Mn–Cr–C alloys [11,12]. It is generally reported that the stacking fault energy decreases with decreasing temperature and aluminum content in Fe–Mn–Cr–C and Fe–Mn–Al alloys [12,13]. The tendency to form ε-martensite increases, while the tendency to form deformation twins decreases with decreasing temperature and aluminum content [13]. Therefore, it is necessary to calculate the stacking fault energy with varying aluminum content and deformation temperature in order to analyze the tendency to form the strain induced features.

According to the Olson's thermodynamic model [14], the stacking fault energy of austenite phase could be expressed as following Eq. (1),

$$\gamma = 2\rho\Delta G^{\gamma-\varepsilon} + 2\sigma \quad (1)$$

where ρ is the density of atoms in a close packed plane in moles per unit area, $\Delta G^{\gamma-\varepsilon}$ is the difference of molar free energy between FCC(γ) and HCP(ε) phases, and σ is the coherent interfacial energy between FCC(γ) and HCP(ε) phases. The coherent interfacial energy, σ, of 10 mJ m^{-2}, reported for the austenitic Fe–Cr–Ni alloys [10], was used to calculate the stacking fault energies of Fe–32Mn–12Cr–xAl–0.4C alloys. Table 3 shows the calculated stacking fault energies and the observed strain induced features in 0-Al, 1-Al and 2-Al at 25°C. The 1-Al alloy with stacking fault energy of 51.7 mJ m^{-2} showed the deformation twins, while the 2-Al alloy with stacking fault energy of 59.9 mJ m^{-2} did not showed the deformation twins. However, the 3-Al alloy, which contains higher aluminum content than the 2-Al alloy, showed the deformation twins after tensile test at 25°C. The presence of deformation twins in 3-Al alloy was found to be closely related with the δ-ferrite phase. The 3-Al alloy contains about 18% of δ-ferrite phase in volume fraction. Since the solubility of aluminum in δ-ferrite phase is much higher than that in austenite phase, the aluminum content in austenite phase of 3-Al alloy becomes much lower than the analyzed content. The exact content of aluminum in austenite phase of 3-Al alloy was analyzed 1.7 wt.% by

Table 2
The existing phases analyzed from the X-ray diffraction of Fe–32Mn–12Cr–xAl–0.4C alloys before and after tensile test at 25, −130 and −196°C

Alloy	Temperature					
	25°C		−130°C		−196°C	
	Before test	After test	Before test	After test	Before test	After test
0-Al	γ	γ	γ	γ	γ	$\gamma+\varepsilon$
1-Al	γ	γ	γ	γ	γ	γ
2-Al	γ	γ	γ	γ	γ	γ
3-Al	$\gamma+\delta$	$\gamma+\delta$	$\gamma+\delta$	$\gamma+\delta$	$\gamma+\delta$	$\gamma+\delta$

γ is the austenite phase, ε is the strain induced martensite phase and δ is the ferrite phase.

wave-length dispersive spectroscopy. The stacking fault energy calculated base on the aluminum content in austenite phase is 56.3 mJ m^{-2} at 25°C, which is smaller than 59.9 mJ m^{-2} in 2-Al alloy. From the calculation of stacking fault energies, it is considered that the deformation twins are formed when the stacking fault energy is below a critical value of about 60 mJ m^{-2}.

Assuming that the stacking fault energy decreases linearly with decreasing temperature by the amount of 0.08 mJ m^{-2} per degree as reported in Fe–Mn–Cr–C alloy [12] and Fe–Cr–Ni alloys [15], the stacking fault energies of Fe–32Mn–12Cr–xAl–0.4C alloys were calculated at various temperatures. The stacking fault energy of 0-Al alloy was calculated as 21.7 mJ m^{-2} at −196°C, while the stacking fault energy of 1-Al alloys was calculated as 34.0 mJ m^{-2} at −196°C. These results agree with the previous result that the formation of strain induced ε-martensite was predominant when the stacking fault energy is below about 20 mJ m^{-2} in Fe–Mn–Cr–C alloys [16].

4. Mechanical properties

The variation of yield strength, ultimate tensile strength of the Fe–32Mn–12Cr–xAl–0.4C alloys with varying temperature are shown in Fig. 3. The yield strength and ultimate tensile strength increased with decreasing temperature from 25 to −196°C. However, the differences on tensile strength and yield strength with varying Al content are negligible. The variation of tensile elongation of the alloys with varying Al content at −196 and 25°C are shown in Fig. 4. The tensile elongations at 25°C decreased with increasing Al content, while the tensile elongation at −196°C decreased with increasing Al content up to 2.1 wt.% and increased at 2.6 wt.%. The 2-Al alloy showed the lowest tensile elongation at 25 and −196°C. Any evidence on dynamic strain aging as serrated stress–strain curve or negative strain rate dependence of flow stress was not observed at temperature ranging from −196 to 25°C.

The tensile elongation of Fe–32Mn–12Cr–xAl–0.4C alloys were closely related to the formation of deformation twins during deformation and were explained as follows. A large uniform elongation of an alloy can be achieved so long as the local necking is retarded during tensile deformation. When a local neck is started at a certain position of specimen, the strain induced deformation twins are preferentially formed near the local neck. As the twin boundaries are the strong barriers to subsequent dislocation motion, the deformation twinning leads to a rapid strain hardening [17,18]. The further propagation of local neck could be retarded by the strain hardening due to the preferential formation of deformation twins near the local neck. Then another neck would start at another position and the propagation of the new neck would be retarded again by the deformation twining. This repeated process of local necking and retardation of its propagation by deformation twinning leads to a multiple necking distributed in the gauge section of specimen, which results in a large uniform elongation [4]. The 2-Al alloy, which did not form the deformation twins showed lowest tensile elongation at 25 and −196°C as shown in Fig. 4. As the formation of deformation twins during tensile deformation leads to a rapid strain hardening, the strain hardening exponent would increase with increasing strain if the deformation twins are formed. Kim et al. [19] reported that the strain hardening exponent of Fe–25Mn–5Ni–5Al–0.3C alloy increased with the formation of deformation twins during tensile deformation. Fig. 5 showed the variations in the strain hardening exponent with varying strain in 0-Al, 1-Al and 2-Al alloys at 25°C. The strain hardening exponent of 2-Al alloy, which did not form the deformation twins, was low and kept almost constant with increasing the strain, while those of 0-Al and 1-Al alloys increased continuously with increasing strain at 25°C. These results indicate that the deformation twins induced the strain hardening effect and increased the strain hardening exponent with increasing strain in 0-Al and 1-Al alloys.

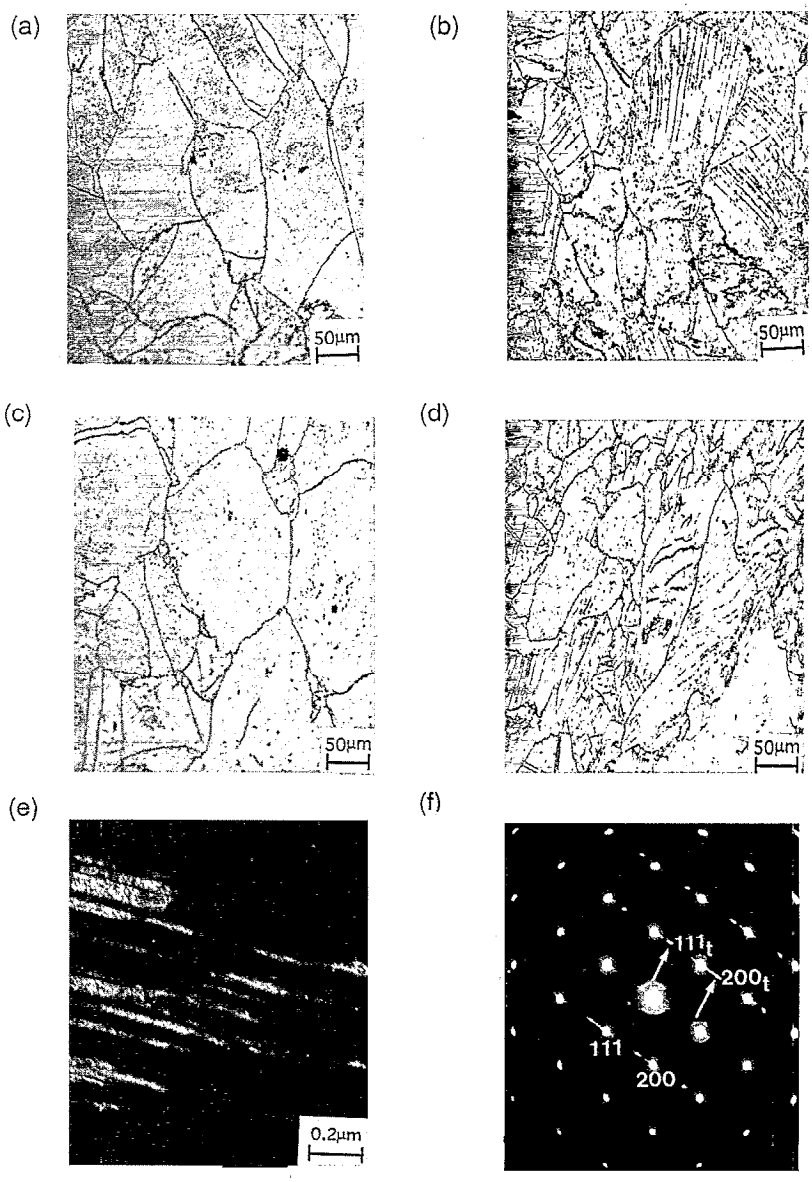

Fig. 2. The microstructures of Fe–32Mn–12Cr–(0, 1)Al–0.4C alloys observed before and after tensile test at 25°C: (a) 0-Al alloy before tensile test, (b) 0-Al alloy after tensile test, (c) 1-Al alloy before tensile test, (d) 1-Al alloy after tensile test, (e) dark field image of deformation twinning after tensile test of 0-Al alloy, (f) electron diffraction pattern from the dark field image of deformation twins with [011] zone axis. The subscript t indicates the twinning spot.

In order to investigate the effect of deformed microstructure on the tensile elongation in 0-Al and 1-Al alloys, the tensile tests were performed at various temperatures ranging from −196 to 250°C. Fig. 6 showed the deformed microstructures and tensile elongation of 0-Al and 1-Al alloys with varying temperature. Fig. 6 can be divided into three regimes based on the observation of deformed microstructure. Both the ε-martensite and deformation twins were observed in regime I. Only the deformation twins were observed in regime II. While, no strain induced phase was observed in regime III. The elongation peaks were observed at intermediate temperature in regime II, in which the deformation twins were formed. The elongation increased at lower temperature when the ε-martensite was formed in addition to the deformation twins in regime I. The elongations were lower when the deformation twins were not formed at higher temperature in regime III. The elongation peak moved toward lower temperature when aluminum content increased as shown in Fig. 6. In the previous research on Fe–26Mn–xAl alloys [6], it was also reported that the elongation peak moved toward lower temperature when aluminum content increased. As mentioned above, assuming that the stacking fault energy decrease linearly with decreasing temperature by the amount of 0.08 mJ m^{-2} per degree, it is considered

Table 3
The calculated stacking fault energies and strain induced phases in Fe–32Mn–12Cr–xAl–0.4C alloys observed after tensile test at 25°C

Alloy	Stacking fault energy at 298 K (mJ m^{-2})	Strain induced phases
0-Al	40.6	Deformation twins
1-Al	51.7	Deformation twins
2-Al	59.9	None
3-Al	56.3	Deformation twins

that the deformation twins are formed when the stacking fault energy values are roughly between 20 and 50 mJ m^{-2} in regime II.

Fig. 7 showed the variation of the strain hardening exponent of 0-Al alloy with varying strain at various temperatures. The strain hardening exponent was low and kept almost constant with increasing strain at 250°C in regime III, which is similar to that of 2-Al alloy at 25°C. The strain hardening exponent increased continuously with increasing strain up to about 0.45 at −10°C in regime II. These results indicate that the deformation twinning induced the strain hardening effect and resulted in an rapid increase of the strain hardening exponent with increasing strain in regime II.

The 0-Al alloy exhibited a peak elongation around −10°C in regime II as shown in Fig. 6. As the amounts of deformation twins in deformed specimens were almost constant as about 10 vol.% with varying temperature, the presence of elongation peaks was considered

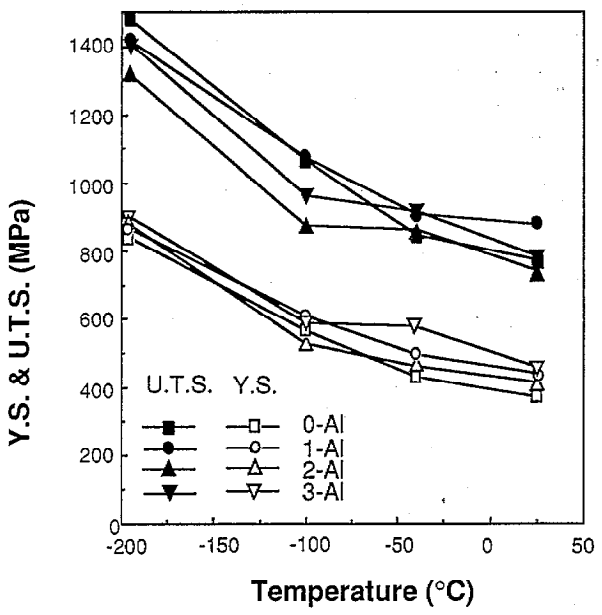

Fig. 3. The variation of ultimate tensile strength and yield strength of Fe–32Mn–12Cr–xAl–0.4C alloys with varying temperature.

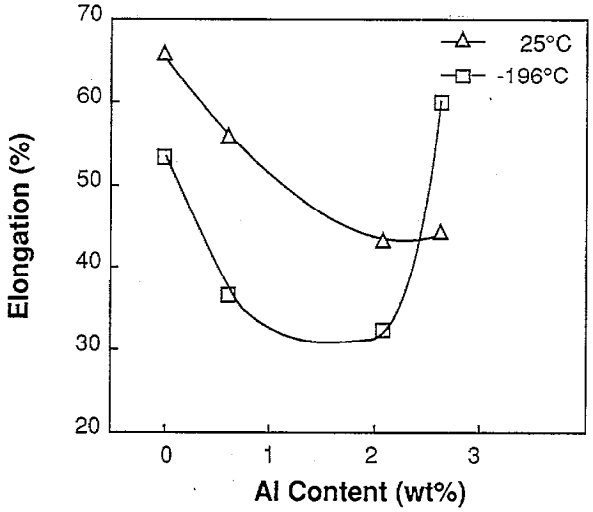

Fig. 4. The variation of elongation of Fe–32Mn–12Cr–xAl–0.4C alloys with varying aluminum content.

to be related to the deformation twinning rate. It is reported that the rate of deformation twinning increased with decreasing temperature, and the peak elongation was obtained at temperature when the rate of deformation twinning was adequate [8]. Fig. 7 compares the strain hardening behavior of 0-Al alloy at −10 and −100°C in regime II. The continuous increase of strain hardening exponent with increasing strain at −10°C represents that the deformation twins were continuously formed up to a strain of about 0.45. On the other hand, the strain hardening exponent increased up to a smaller strain of about 0.15 and then decreased at −100°C indicating that the formation of deformation twins were completed at the early stage of deformation. These results represent that a gradual formation of deformation twins up to a large strain is advantageous to enhance the tensile elongation.

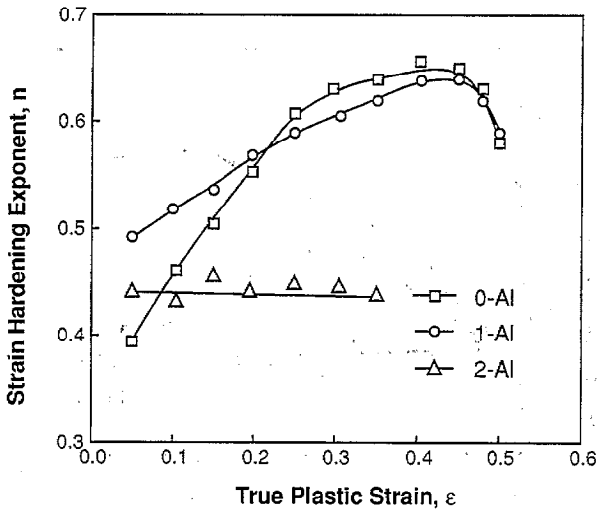

Fig. 5. The variation of strain hardening exponent of Fe–32Mn–12Cr–(0, 1, 2)Al–0.4C alloys with varying true plastic strain at 25°C.

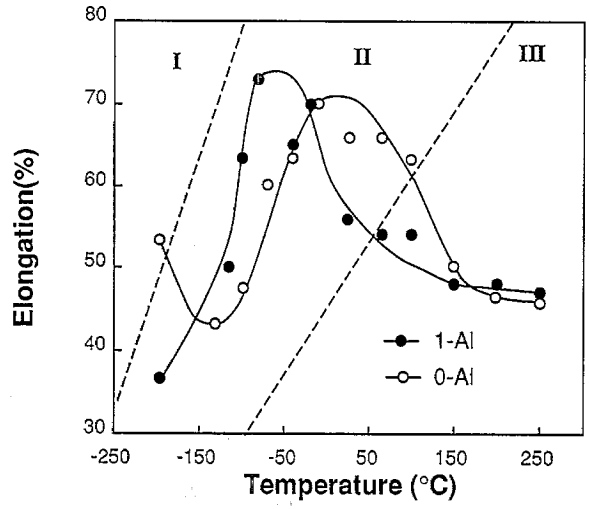

Fig. 6. The variation of elongation and deformed microstructures of Fe–32Mn–12Cr–(0, 1)Al alloys with varying temperature. The deformation twins and ε-martensite were observed in regime I, only deformation twins were observed in regime II and no strain induced features were observed in regime III.

The effect of the strain induced ε-martensite on tensile elongation was not clearly explained in previous research on high manganese austenitic alloys [6,11], because the effect of the formation of strain induced ε-martensite often mixed with that of deformation twins. The tensile elongation of 0-Al alloy increased at −196°C in regime I, where the strain induced ε-martensite was observed in addition to the deformation twins, as shown in Fig. 6. Since the only difference in microstructure is the presence of ε-martensite at −196°C, this result clearly indicates the formation of ε-martensite is also beneficial to increase the tensile elongation. The strain induced ε-martensite was also preferentially formed around a neck [20–23]. It is considered to retard the neck propagation similar as the deformation twins. The variation of the strain hardening exponent with varying strain at −196°C in regime I is shown in Fig. 7. Even though the rate of deformation twinning at −196°C is expected to be much faster than that at −10°C, the strain hardening exponent increased continuously with increasing strain up to about 0.45 at −196°C similar to that at −10°C. This increase of the strain hardening exponent with increasing strain at −196°C is considered due to the additional effect of the gradual formation of the strain induced ε-martensite during deformation. These observations represent that the formation of strain induced ε-martensite also enhances the tensile elongation of 0-Al alloy as the same manner as deformation twinning and would be more important at lower temperature below −150°C.

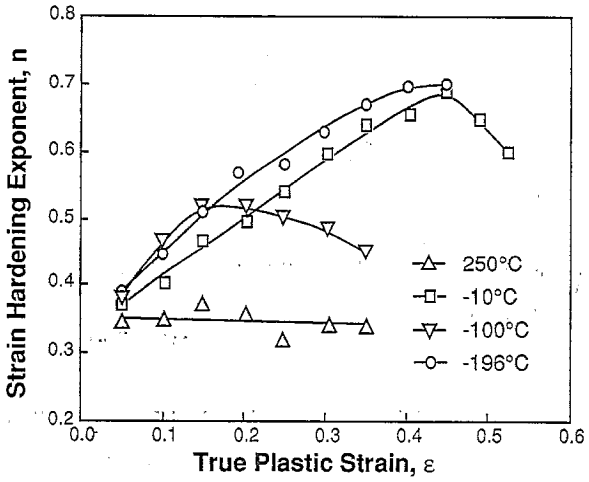

Fig. 7. The variation of strain hardening exponent of Fe–32Mn–12Cr–0Al–0.4C alloy with varying true plastic strain.

5. Conclusions

The effects of Al addition (0–3 wt.%) to Fe–32Mn–12Cr–xAl–0.4C cryogenic alloys on tensile properties and microstructures were investigated from −196 to 250°C and the major conclusions are outlined below.

(1) In Fe–32Mn–12Cr–xAl–0.4C alloys, the aluminum behaved as an austenite stabilizer against the ε-martensite formation when added up to 0.6 wt.%, while behaving as a δ-ferrite forming element when added above 2.6 wt.%.

(2) The strain induced deformation twinning was observed in deformed cryogenic Fe–32Mn–12Cr–xAl–0.4C alloys if the stacking fault energy of austenite phase is below about 60 mJ m^{-2}. The ε-martensite was only observed in deformed Fe–32Mn–12Cr–0Al–0.4C alloy at −196°C with the stacking fault energy of 21.7 mJ m^{-2}.

(3) The tensile deformation behavior of Fe–32Mn–12Cr–0Al–0.4C cryogenic alloy with varying temperature was divided into three regimes on the formation of strain induced features during the deformation. Both deformation twins and ε-martensite were formed in regime I below about 150°C. Only deformation twins formed in regime II between −150 and 150°C. No strain induced features were observed in regime III above 150°C. The peak elongation of 70% was obtained in region II.

(4) The formation of both the deformation twins and ε-martensite enhanced the tensile elongation by retarding a local necking. The continuous formation of deformation twins up to a large strain was advantageous to enhance the tensile elongation.

References

[1] R.P. Reed and A.F. Clark, *Materials at Low Temperatures*, ASM, 1983, pp. 371.

[2] J.P. Bruner and D.A. Sarno, *Adv. Cryog. Eng.*, *24* (1978) 529.
[3] J. Charles, A. Berghezan, A. Lutts and P.L. Dancoisne, *Met. Prog.*, May (1981) 71.
[4] Y.G. Kim, Y.J. Park and J.K. Han, *Metall. Trans. A*, *16* (1985) 1689.
[5] Y. Tomota, M. Strum. and J.W. Mowis, Jr., *Metall. Trans. A*, *17* (1986) 537.
[6] Y.G. Kim, J.M. Han and J.S. Lee, *Mater. Sci. Eng.*, *A114* (1989) 51.
[7] Soon H. Hong and Young S. Han, *Scripta Metall.*, *53* (1995) 1489.
[8] J.M. Han, C.Y. Lim and Y.G. Kim, *Acta Metall.*, *39* (1991) 2169.
[9] K. Sato and M. Ichinose, *ISIJ Int.*, *29* (1989) 868.
[10] L. Remy, *Acta Metall.*, *26* (1978) 443.
[11] F. Lecroisey and A. Pineau, *Metall. Trans.*, *3* (1972) 387.
[12] L. Remy and A. Pineau, *Mater. Sci. Eng.*, *A28* (1977) 99.
[13] W.S. Yang and C.M. Wan, *J. Mater. Sci.*, *25* (1990) 1821.
[14] G.B. Olson and M. Cohen, *Metall. Trans. A*, *7* (1976) 1897.
[15] R.M. Latanision and A.W. Ruff, Jr., *Metall. Trans.*, *2* (1971) 505.
[16] P.H. Adler, G.B. Olson and W.S. Owen, *Metall. Trans. A*, *17* (1986) 1725.
[17] K.S. Ragharam, A.S. Sastri and M.J. Marchinkowski, *Trans. AIME*, *245* (1969) 1569.
[18] L. Remy, *Metall. Trans. A*, *12* (1981) 387.
[19] Y.G. Kim and C.Y. Lim, *Metall. Trans. A*, *19* (1988) 1625.
[20] R.G. Stringfellow, D.M. Parks and G.B. Olson, *Acta Metall.*, *40* (1992) 1703.
[21] H. Fujita and S. Ueda, *Acta Metall.*, *20* (1972) 759.
[22] G.B. Olson and M. Cohen, *Metall. Trans. A*, *13* (1982) 1907.
[23] G.B. Olson and M. Cohen, *Metall. Trans. A*, *6* (1975) 791.